Hindawi
Shock and Vibration
Volume 2021, Article ID 8833460, 15 pages
https://doi.org/10.1155/2021/8833460

Research Article

Experimental Research on Vibration Reduction of Cantilever Structure in High-Temperature Environments

Di Jia,[1] Fuhao Peng,[2] Tao Zhou ,[1] Xueren Wang,[1] Qingliang Lu,[1] and Yiwan Wu [2]

[1]*Naval Research Academy, Beijing 100161, China*
[2]*Engineering Research Center for Metal Rubber, School of Mechanical Engineering and Automation, Fuzhou University, Fuzhou 350116, China*

Correspondence should be addressed to Tao Zhou; zhoutaobeijing@outlook.com

Received 25 September 2020; Accepted 18 December 2020; Published 4 January 2021

Academic Editor: Yingtao Tian

To reduce the vibration of a cantilever steel plate in high-temperature environments (25°C–500°C), a new composite structure with entangled metallic wire material (EMWM) core was proposed. The damping performance of the EMWM under different temperatures was investigated. The results show that when the temperature does not exceed 260°C, the damping property of the EMWM is not affected by temperature. When the temperature exceeds 260°C, the damping property of the EMWM decreases with the increase of temperature. A thermal-vibration joint test system was set up to verify the energy dissipation mechanism of the composite structure with EMWM core and to research the effect of vibration reduction under different temperatures. The displacement deviation between the baseplate (steel plate) and constraining plate was sufficient to cause frictional energy dissipation of the EMWM core. The thermal-vibration joint test results indicated that the EMWM core had a positive impact on the damping properties of the cantilever structure. Adding EMWM core and constraining plate can significantly increase the damping ratio and reduces the vibration of the cantilever structures under different temperatures. This research is helpful to control the structural vibrations of cantilever structures in high-temperature environments.

1. Introduction

The reduction of structural vibration amplitudes in the mechanical system has currently become a key objective in many industrial sectors to extend the life of components, reduce acoustic radiation, or increase comfort and security [1]. Cantilever structures are widely used in various fields, such as the wing structure of high-speed flight vehicle. Unlike the multiends clamped structure, the cantilever structure has a large vibration amplitude due to fewer boundary constraints.

There are different techniques aimed at the vibration reduction of plate-structures [1]. Passive surface treatment using various polymer damping materials is the most common damping technique. It is generally accepted that the damping material used in the form of constrained layer damping treatment is most effective. However, it should be noted that most of the traditional polymer damping materials and adhesive (such as epoxy resin) cannot work normally for a long time in the high-temperature environment, especially over 260°C.

Entangled metallic wire material (EMWM) is a kind of porous damping material made from various metallic wires by coiling, weaving, and molding [2]. Although some researchers prefer to use the term metal rubber (MR) [3–6] or metal wire mesh [7, 8], the manufacturing processes of these materials are highly similar, so they are the same kind of material [9].

Because of its excellent energy absorption and environmental adaptability, EMWM has triggered numerous research studies in recent decades [10–13]. Xiao et al. investigated the vibration reduction of high-temperature pipeline system by adding an EMWM coating layer [10]. Zhu et al. proposed a new composite foundation by adding EMWM layer to a rigid foundation [11]. Their research results show that EMWM can effectively reduce the vibration of the foundation between

room temperature and 300°C. Hou et al. noted that, in a wide temperature range (−70°C to 300°C), entangled metallic wire material has excellent damping performance with loss factor about 0.2–0.3, and its damping capacity exhibits good resistance of high-low temperature [12]. Li and Bai investigated the compressive property of knitted-dapped metal rubber at different temperatures (25, 100, 200, and 300°C) and reported that the stiffness and damping of the specimen decreased and then increased with the increase of temperature [13].

Previous researches have shown that EMWM can work normally under high temperature. It means that the EMWM can be used for vibration reduction design of cantilever structures in high-temperature environments. Therefore, to improve the damping performance of cantilever structure in the wide temperature range, an additional EMWM layer can be mounted to such structure. As illustrated above, the adhesive cannot be used to bond EMWM with cantilever structure under high temperature. But a mechanical connection is a potential solution. Then, the mechanism of vibration reduction will be different from the traditional Sandwich structure with a viscoelastic core.

The methods for constructing a simulated thermal environment are airflow heating and radiant heating [14]. Radiant heating has the advantages of long heating time, strong heating capacity, multitemperature zone control, etc. Thus, the radiant heating method was widely used in thermovibration joint test [14, 15]. Ding et al. set up a transient aerodynamic heating environment simulation system by using two quartz lamp arrays and investigated the thermal modal characteristics of a ship's foundation under 300°C. To reduce costs and avoid signal compensation, ceramic rods are often used to induce the vibration response signal of the structure at high temperature to room temperature for data collection [14, 15].

The main aim of this paper is to investigate the vibration reduction of cantilever structure by adding entangled metallic wire material core in a wide ambient temperature from room temperature (25°C) to 500°C. The damping properties of the EMWM were evaluated through a series of quasi-static compression tests. To research the thermal characteristics of the cantilever structure, a thermal-vibration joint test system was set up. The damping mechanism and the modal characteristics of the new cantilever structure were studied by the thermal-vibration joint test system. Furthermore, the effect of vibration reduction was assessed in high-temperature environments.

2. Composite Cantilever Structure

2.1. Entangled Metallic Wire Material. In this paper, the EMWM specimens were manufactured using 304 (0Cr18Ni9) stainless steel wires following a four-step process, as that adopted by Bai et al. [2], Gadot et al. [16], and Ma et al. [17]. ①The ordinary wire is encircled into a tight helix according to the processing principle of the helix spring. ②The tight helix is stretched and weaved in a crisscross pattern to obtain a rough porous base material. ③The rough samples are placed into a specially designed mold and shaped into final form by applying a compressive force to obtain a primary EMWM. ④The primary EMWM samples are postprocessed (such as ultrasonic clean) to obtain the final EMWM. Tables 1 and 2 present the chemical composition and mechanical performance of the 304 stainless wire, respectively. The diameter of the wire is 0.3 mm, the spring diameter of the wire helix is 3.5 mm, and the helix angle is 60°. To assess the repeatability of the results, five specimens with the same preparation parameters were prepared, as shown in Table 3. The prepared plate-like EMWM specimen is shown in Figure 1.

2.2. Composite Cantilever Structure with EMWM Core. Figure 2(a) is the sketch of a typical composite structure with a viscoelastic core. To reduce the vibration of the baseplate, a viscoelastic core and a constraining plate were bonded to the baseplate using adhesive (such as epoxy resin). When the baseplate is excited, the vibration energy will be dissipated through shear deformation of viscoelastic materials. As ambient temperature increases, the mechanic performance of the viscoelastic core and adhesive will decrease gradually and drop sharply at high temperature.

Figure 2(b) is the sketch of a new composite structure with EMWM core. To ensure that the EMWM can be reliably connected with the baseplate and constraining plate in high-temperature environments, the baseplate, EMWM layer, and constraining plate are mounted together by rivets or bolts. The positioning of the plates is ensured by limit blocks. When the baseplate is excited, the baseplate and constraining plate will produce displacement response, respectively, and the deviation in the displacement between the baseplate and constraining layer will change the compression state of the EMWM layer, the vibration energy will be dissipated through friction between adjacent wire helixes in contact. The proposed composite structure with EMWM core is a pure metal structure, which makes it possible to reduce the structure vibration in high-temperature environments.

The detail sizes of the baseplate are shown in Figure 3. The shadow area of the baseplate is clamped, and the remaining area is damped to increase the damping performance of the structure by adding EMWM layer and constraining plate. The thickness of the base plate is 8 mm. The size of the constraining layer is $150 \times 150 \times 3\ \text{mm}^3$. The material of the baseplate, constraining plate, and limit blocks are 45 steel. The thermophysical properties of the 45 steel are shown in Table 4. Desu et al. reported that, for austenitic stainless steel, the strength drops almost 30% by increasing the temperature from 50°C to 500°C [18].

To obtain the dynamic characteristics of the cantilever baseplate, 12 measuring points are arranged on the baseplate, an excitation point is located at the center of the baseplate, 2 temperature monitoring points are arranged on the baseplate, and 4 connection points (M6 threaded holes) are arranged on the baseplate. The layout of measuring points (point D1~D12), excitation point (point A), temperature monitoring points (points T1 and T2), and connection points (point B1~B4) are shown in Figure 3. The inner diameter, outer diameter, and height of the limit block

Table 1: Chemical composition (wt.%) of 304 stainless wire.

Chemical element	Cr	Ni	Mn	Si	C	S	*P*	Fe
Percentage	17/19	8.0/11.0	≤2.0	≤1.0	≤0.07	≤0.03	≤0.035	Balance

Table 2: Mechanical performance of 304 stainless wire.

Tensile strength (MPa)	Yield strength (MPa)	Elongation δ%	Section shrinkage (%)	Brinell Hardness HB
≥520	≥205	≥40	≥60	≦187

Table 3: The dimensions and structure parameters of EMWM samples.

Specimen	Height (mm)	Width (mm)	Length (mm)	Mass (g)	Forming pressure (kN)	Density (kg/m3)
EMWM-1	8.03	150.2	150.3	396	164.5	2200
EMWM-2	8.07	150.1	150.2	396	164.4	2200
EMWM-3	8.06	150.2	150.4	396	164.3	2200
EMWM-4	8.02	150.2	150.1	396	164.3	2200
EMWM-5	7.96	150.1	150.3	396	164.4	2200

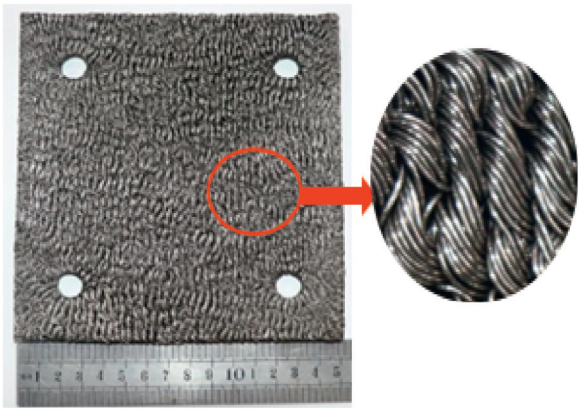

Figure 1: Picture of platelike EMWM specimen.

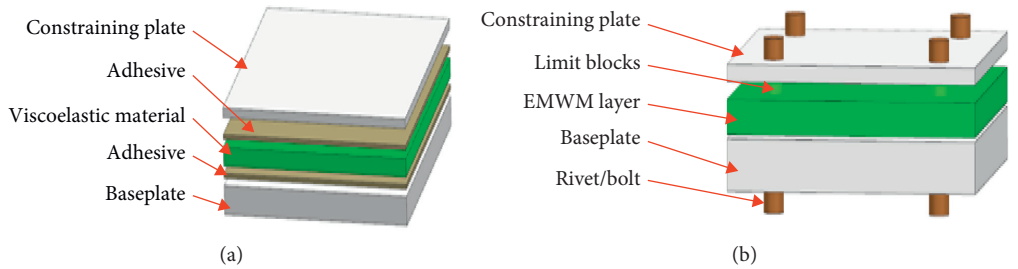

Figure 2: Sketches of two kinds of composite structures. (a) Composite structure with viscoelastic core. (b) Composite structure with EMWM core.

are 6.2 mm, 10 mm, and 6 mm, respectively. Therefore, the amount of preload for each EMWM specimen is 2 mm. The constrained area of the baseplate is clamped by a constraint beam and bolted to supporting base. The cantilever composite structure with EMWM core is shown in Figure 4.

3. Experimental Devices and Methods

3.1. Quasi-Static Test. To obtain the stiffness and damping characteristics of EMWM under different ambient temperatures, a series of quasi-static test were carried out using a

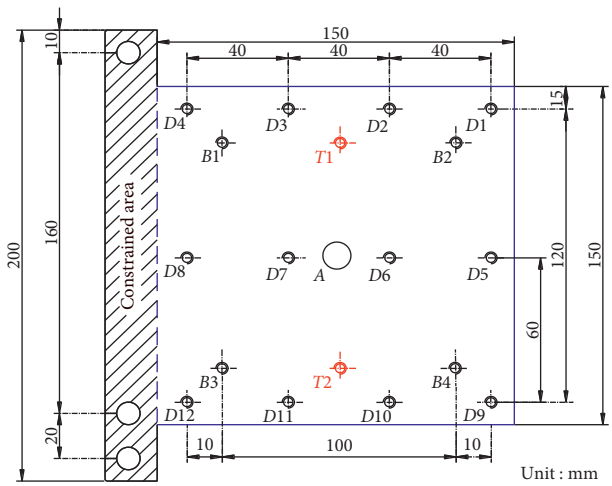

Figure 3: Dimensions of the baseplate.

Table 4: Thermophysical properties of the 45 steel.

Temperature (°C)	Density $\rho/(kg{\cdot}m^{-3})$	Thermal conductivity $k/(W{\cdot}m^{-1}{\cdot}K^{-1})$	Specific heat capacity $c/(J{\cdot}kg^{-1}{\cdot}K^{-1})$	Poisson's ratio ν	Coefficient of expansion $\alpha/(\mu{\cdot}K^{-1})$	Modulus of elasticity E/GPa
20	7850	55	465	0.3	1.1	206
250	7800	55	470	0.3	1.21	175
500	7650	55	490	0.3	1.37	130

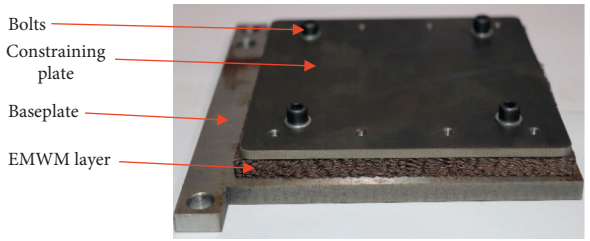

Figure 4: Image of the cantilever composite structure with EMWM core.

WDW-T200 electronic universal testing machine and a high-temperature testing box. Figure 5 shows the quasi-static test device. This test device was manufactured by Jinan Tianchen Testing Machine Manufacturing Co., Ltd. The parameters of the quasi-static test device are as follows: the maximum compression force is 200 kN, the maximum temperature is 800°C, the displacement resolution is 0.001 mm, the load resolution is 1N, and the temperature resolution is 1°C.

The WDW-T200 was used in displacement-control mode. During each test, the loading and unloading speed were controlled at 1 mm/min. Quasi-static tests were carried out at room temperature (25°C), 100°C, 200°C, 260°C, 300°C, 400°C, and 500°C, respectively.

In this paper, secant stiffness (k) and loss factor (η) were used to evaluate the stiffness and damping performance of EMWM, respectively. The secant stiffness and loss factor can be derived from the quasi-static hysteresis loop of the EMWM. Figure 6 presents the sketch of the hysteresis loop under the loading and unloading process. The secant stiffness (k) is a measure of the ratio of the maximum loading force (F_{max}) divided by the maximum deformation (d_{max}) of the EMWM, as shown in (1). Due to the existence of sliding friction between adjacent metal wire helixes, the loading and unloading curve do not coincide. ΔW is the area between loading and unloading curve and is used to represent the dissipated energy in per cycle. U is the sum of the area under the unloading curve and half of ΔW and is used to represent the maximum elastic potential energy in per cycle. The loss factor is defined as (2).

$$k = \frac{F_{max}}{d_{max}}, \tag{1}$$

$$\eta = \frac{\Delta W}{\pi U}. \tag{2}$$

The EMWM will not deform plastically when the maximum loading force does not exceed about 20% of the maximum forming pressure. Considering the maximum forming pressure of each specimen was about 164 kN, the maximum loading force was set as 35 kN. To prevent the uneven contact surface between the specimens and the test holders, a 10N precompression is applied to each specimen. After molding, the internal wire helixes of EMWM connect with each other and form a stable structure. However, there are still some wire helixes which are in a critical state of being unstable. Figure 7 shows the first five cyclic force-displacement cures of EMWM-1. It can be seen from Figure 7 that the first hysteresis loop is significantly different from the others, and then the performance of EMWM will be stable after multiple loading. Thus,

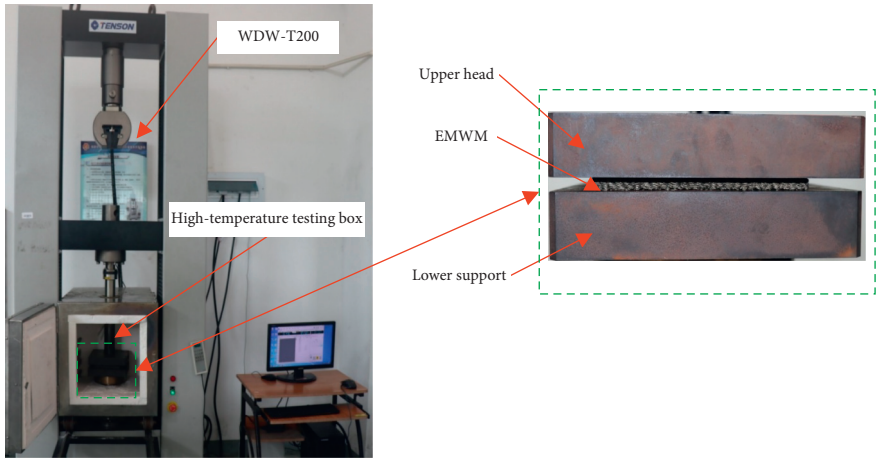

Figure 5: Quasi-static test device.

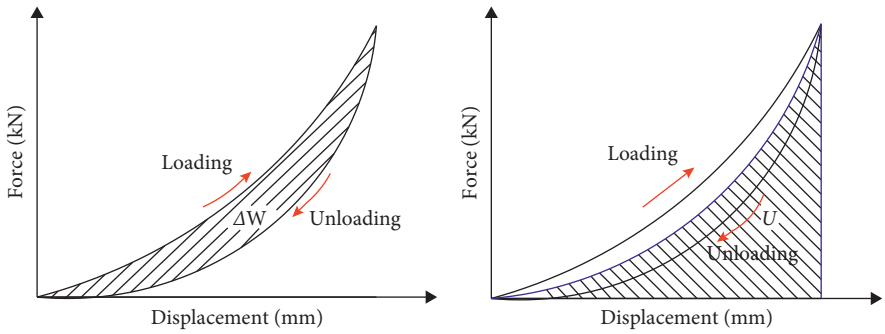

Figure 6: Sketch of the hysteresis loop.

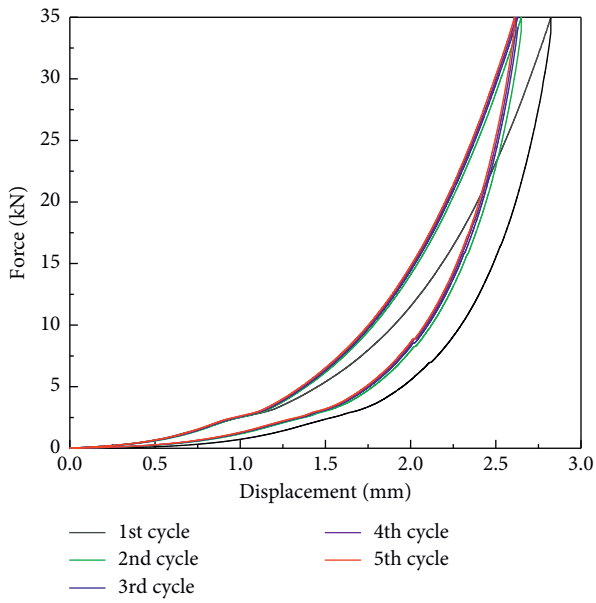

Figure 7: Cyclic force-displacement curves (EMWM-1, 25°C).

the experimental data of the 5th hysteresis loop was used to evaluate the quasi-static properties.

3.2. Thermal-Vibration Joint Test. A thermal-vibration joint test system was setup to evaluate the vibration reduction of cantilever structure in high-temperature environments. Moreover, this system was used to validate the damping mechanism of the composite structure with EMWM core. Figure 8 presents the block diagram of the thermal-vibration joint test system which consists of a thermal environment simulation subsystem and a vibration excitation and acquisition subsystem. The thermal environment simulation subsystem is used to generate the desired high-temperature environment. The vibration excitation and acquisition subsystem is set up for simulating the external load on the cantilever structure and collecting the vibration response signals.

As shown in Figure 9, the cantilever structure is fixed on the supporting base through bolts. Two quartz lamp infrared heating arrays are installed on the top and bottom of the cantilever structure. The distance between the quartz lamp

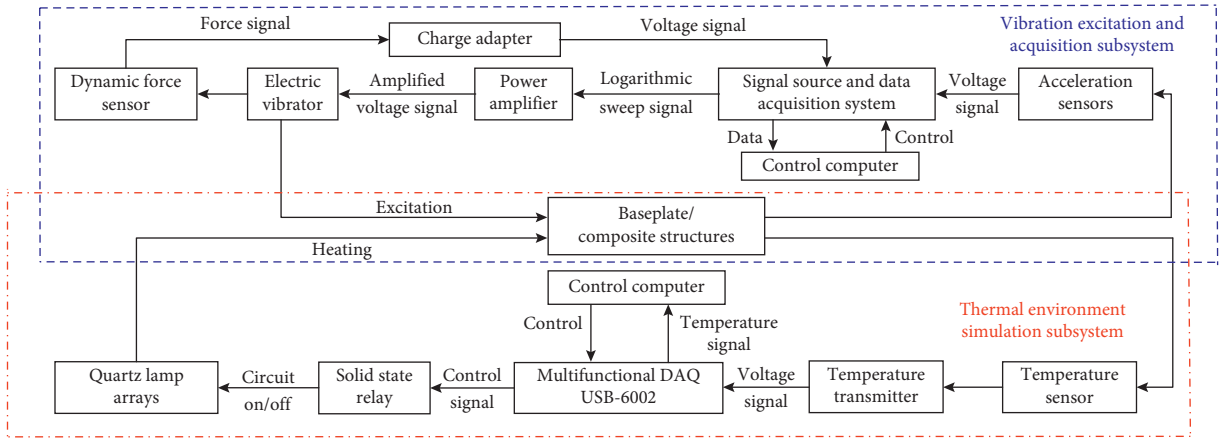

Figure 8: Block diagram of the thermal-vibration joint test system.

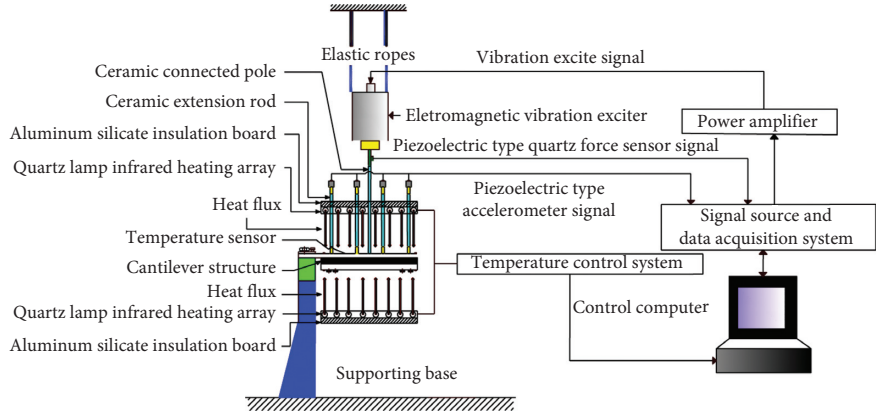

(a)

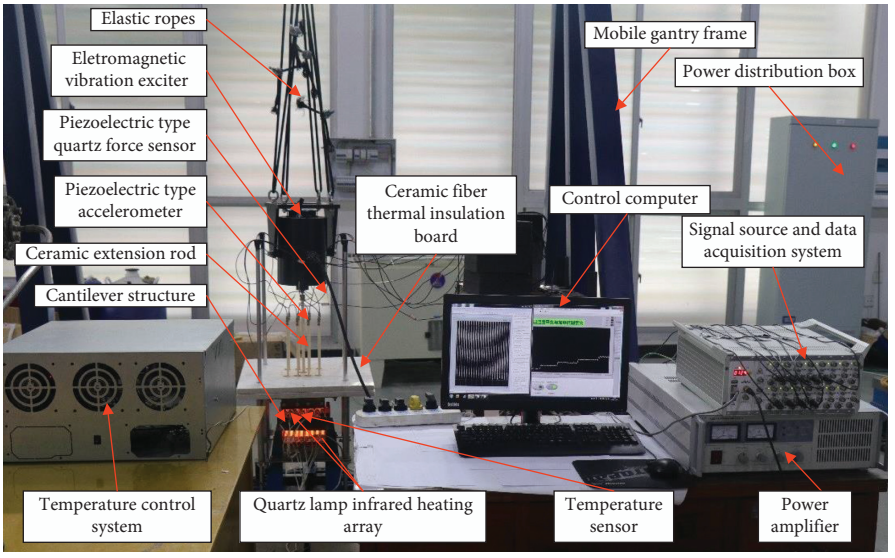

(b)

Figure 9: Thermal-vibration joint test system. (a) Schematic of the experimental modal test system. (b) Photograph of the thermal/vibration joint test.

array and cantilever structure is 30 mm. The electromagnetic vibration exciter is suspended above the cantilever structure through elastic ropes and is connected with the cantilever structure by a ceramic connected pole. An aluminum silicate insulation board is placed between the quartz lamp array and the electromagnetic vibration exciter to provide heat insulation during heating. To reduce the test cost and avoid signal compensation, the high-temperature acceleration sensor is not adopted, but a combination of ordinary acceleration sensor and ceramic extension rod is adopted to acquire the vibration signals of the cantilever structure in a high-temperature environment. Twelve ceramic extension rods are fixed on the measuring points (D1~D12) of the baseplate at one end and connected to the ordinary acceleration sensors at another end by threads. It is noted that these ceramic extension rods pass through the aluminum silicate insulation board to ensure that the ordinary acceleration sensors are within the normal temperature range during heating.

Table 5 presents the technical specifications of the main equipment for the thermal-vibration joint test system. The uT8916FRS-DY was used to generate a sinusoidal sweeping signal in the experimental modal test. On the other hand, it was used to detect the displacement deviations between the baseplate and constraining layer, which can reflect the deformation of the EMWM layer. It also was used to acquire the acceleration signals of the baseplate, which can reflect the modal characteristics of the cantilever structure.

During the thermal-vibration joint test, the baseplate and constraining plate are heated simultaneously by two quartz lamp infrared heating arrays. The thermal environment simulation subsystem is employed to generate a desired high-temperature environment. After keeping the desired temperature for 30 minutes, the electromagnetic vibration exciter sends sinusoidal sweep force to continuously excite the cantilever structure. The parameters of the excitation signal are given in Table 6. The response of the cantilever is detected by the use of twelve ordinary accelerometers. The excitation and response signals are recorded and processed using the vibration excitation and acquisition subsystem in real time.

At the end of the thermal-vibration joint test, the amplitude-frequency curves for the response of the baseplate (steel plate) and composite structure with EMWM core under different ambient temperatures can be acquired. Therefore, the effect of EMWM on the vibration and damping characteristics of this cantilever structure can be obtained. Furthermore, the damping ratio (ξ) of the baseplate (steel plate) and composite structure with EMWM core could be determined by the half-power bandwidth of the response amplitude versus frequency plot.

$$2\xi = \frac{\omega_2 - \omega_1}{\omega_n}, \tag{3}$$

where ω_n is the n order modal frequency of the structure and ω_1 and ω_2 are the half-power point frequencies on the magnification ratio versus frequency ratio plots response curve that have a value of $\sqrt{2}/2$ times the response amplitude at the n order modal frequency.

As mentioned above, this test system was used to validate the damping mechanism of the composite structure with EMWM core. During the modal test, the displacement response of the baseplate and constraining plate are micron scale. As shown in Table 5, the working temperature range of KD9002 was from -20°C~ + 80°C. Moreover, the displacement deviation between the baseplate and constraining layer is very small and the displacement difference was measured only at room temperature. To detect the displacement deviation between the baseplate and constraining layer and ensure the accuracy of the test, the ceramic extension rods and the quartz lamp infrared heating arrays are removed, and then 12 sinusoidal sweep tests were carried out at the same excitation point (point A), a pair of eddy current displacement sensors (KD9002) were used to measure the displacement response of the baseplate and constraining plate at the 12 measuring points (D1~D12), respectively, as shown in Figure 10. The displacement deviations between the baseplate and constraining layer at D1~D12 were detected and recorded by uT8916FRS-DY. The direction of the displacement is positive in the vertical direction, and vice versa.

4. Results and Discussion

4.1. Quasi-Static Behavior under Different Temperatures. Figure 11 shows the quasi-static test results for a specimen (EMWM-1) under different ambient temperatures. The dissipated energy in the per cycle (ΔW), secant stiffness (k), and loss factor (η) of each specimen under different ambient temperatures are presented in Figure 12, together with their mean value (MV) and standard deviation (STD).

It can be seen from Figure 11 that the ambient temperature has a significant effect on the hysteretic path. The hysteretic curves of EMWM at different temperatures can eventually return to the original position. It indicates that, during the quasi-static compression tests under different ambient temperatures (25°C ~ 500°C), no plastic deformation occurred, and the maximum loading force (35 kN) did not exceed the maximum allowable load of the specimens.

As illustrated in Figures 11 and 12(a), with the ambient temperature increase from 25°C to 260°C, the dissipated energy in one cycle through friction between adjacent wire helixes decreases slightly. However, when the temperature is greater than 260°C, as the temperature continues to rise, the amount of dissipated energy in one cycle will decrease rapidly. The changes in sliding friction coefficient and thermal expansion of wire helixes are two main factors leading to this phenomenon. As the ambient temperature increases, an oxidation film will gradually form on the surface of the wire helixes, especially at high temperature (≥260°C), the densification of the oxidation film will be further improved. And then the coefficient of sliding friction between wire helixes decreases with the densification of the oxidation film. Therefore, when the temperature is greater than 260°C, the energy consumption of dry friction will rapidly decrease. Meanwhile, the amount of thermal expansion of the wire helixes will become larger with the increase of temperature. And then the porosity of EMWM

Table 5: Technical specifications of the main equipment for the test system.

No.	Name	Model	Manufacturer	Quantity	Parameters	Value/unit
1	Signal source and data acquisition system	uT8916FRS-DY	uTekl Electronic Technology Co., Ltd. (Wuhan, China)	1	Number of input channels Number of output channels	16 2
2	Electromagnetic vibration exciter	JZQ-50	ECON Technologies Co., Ltd. (Hangzhou, China)	1	Maximum exciting force Maximum displacement	500 N 7.5 mm
3	Power amplifier	E5878	ECON Technologies Co., Ltd. (Hangzhou, China)	1	Maximum output power	1500 W
4	Piezoelectric type quartz force sensor	YD-303	Yangzhou Yixuan Electronic Technology Co., Ltd. (Yangzhou, China)	1	Resonant frequency Charge sensitivity Working temperature range	≥60 KHz 3.08 pC/N −40°C~ + 150°C
5	Eddy current displacement sensors	KD9002	Yangzhou Kedong Electronics Co., Ltd. (Yangzhou, China)	2	Sensitivity Resolution Measuring distance Working temperature range	8 mV/μm 0.4 μm 2 mm −20°C~ + 80°C
6	Piezoelectric-type accelerometer	1A102 E	Jiangsu Donghua Test Technology Co., Ltd. (Jingjiang, China)	12	Sensitivity Measuring range Working temperature range	10.36 mV/g ±500 g −40°C~ + 120°C
7	Quartz lamp	QL-500	Baoda Electrical Appliances Co., Ltd. (Zhejiang, China)	14	Infrared radiation wavelength Power Length	2.3–14 μm 500 W 240 mm

Table 6: Parameters of the excitation signal.

Parameters	Amplitude (N)	Sampling rate (kHz)	Waveform	Sweep mode	Sweep range	Sweep rate
Value	110	5	Sine	Logarithmic	10–500 Hz	1 oct/min

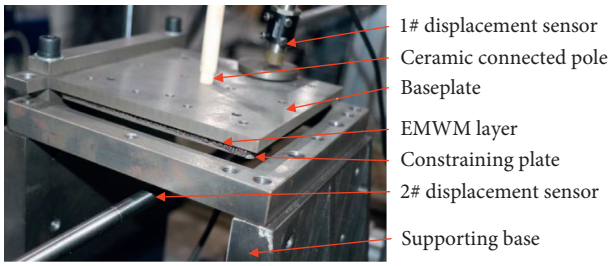

Figure 10: Displacement deviation test system.

will gradually decrease; therefore, the sliding space of the wire helixes inside the EMWM will gradually become smaller and lead to a reduction in energy consumption.

Figure 12(b) shows that the secant stiffness of the EMWM increases with the increase of temperature. This has been explained by authors in recent research [19]. As temperature increased, although the elastic modulus and shear modulus of stainless steel wire will gradually decrease, the amount of thermal expansion of the wire helixes will become larger and then the number of contact points increases; finally, the stiffness characteristic of EMWM is gradually similar to solid structures, and the nonlinear characteristics of the force-displacement curve of EMWM would be weakened [19].

Figure 12(c) presents the loss factor of EMWM under different ambient temperature. It should be noted that the loss factor is a calculated value rather than a direct measurement. According to (2), it is found that the loss factor is proportional to the dissipated energy in one cycle and inversely proportional to maximum elastic potential energy in one cycle. The loss factor of EMWM decreases slightly with the increase of the ambient temperature from 25°C to 260°C, and this result is consistent with that of Hou et al. [12]. It indicates that the loss factor of EMWM has little correlation with the ambient temperature in the range of 25°C–260°C. As shown in Figure 12(a), the dissipated energy in one cycle gradually decreases with the increase of temperature (25°C ~ 260°C). Meanwhile, the maximum elastic potential energy increases gradually with the increase of stiffness characteristics of EMWM material. Therefore, the loss factor decreases slightly at 25°C-260°C. However, when the temperature is greater than 260°C, as the temperature continues to rise, the loss factor will decrease rapidly. This is due to the rapid decrease in energy consumption and the rapid increase in stiffness.

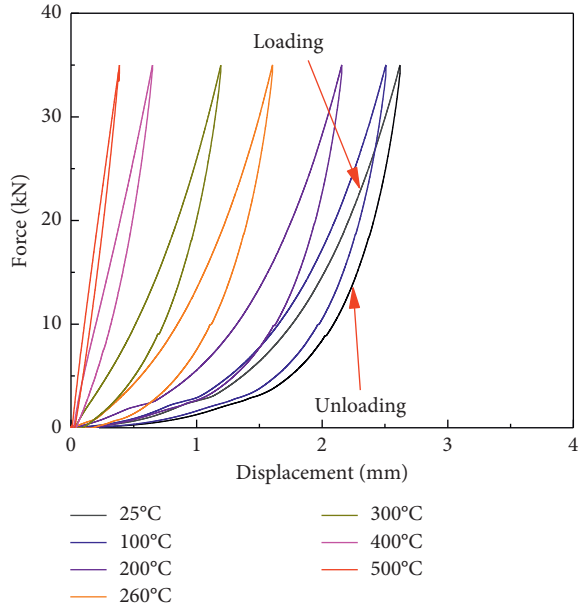

Figure 11: Force-displacement curves of EMWM under different ambient temperature.

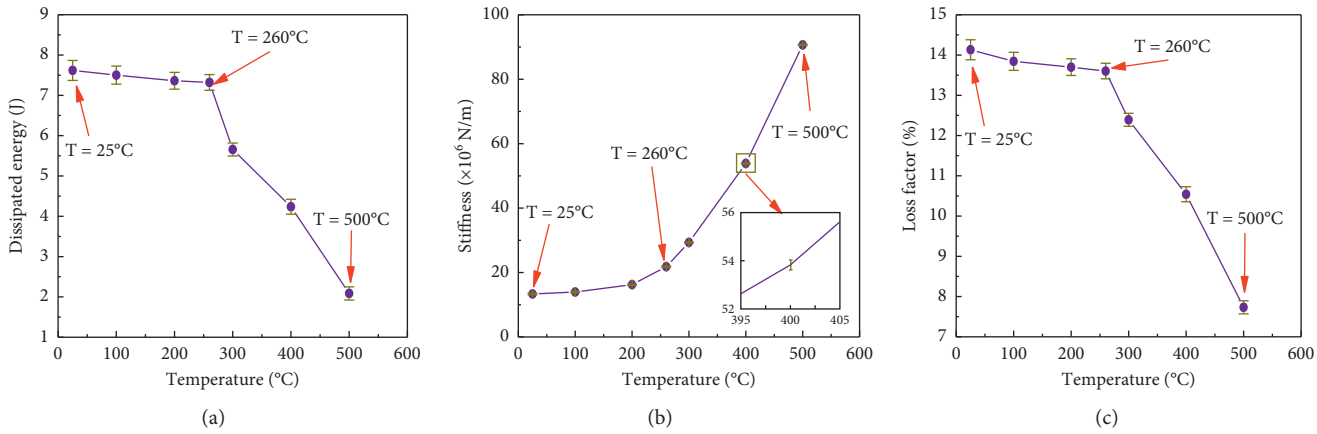

Figure 12: Dissipated energy, secant stiffness, and loss factor of EMWM under different ambient temperature. (a) Dissipated energy in one cycle (ΔW), (b) secant stiffness (k), and (c) loss factor (η).

4.2. Displacement Deviation. To verify the energy dissipation mechanism of the composite structure with EMWM core, the displacement deviation between the baseplate and the constraining layer at different measuring points (D1~D12) was detected at room temperature. The measuring point D1 is near the free end of the cantilever composite structure; thus, the relationship between displacement deviation at D1 and frequency was presented and analysed, as shown in Figure 13. And the maximum displacement deviations of other measuring points will be presented in Table 7.

It can be seen from Table 7 that the maximum displacement deviations of the cantilever composite structure with EMWM core at the first three order modal frequencies were larger than 1 μm. It means that, around the first three order modal frequencies, the displacement deviation between the baseplate and constraining plate can cause frictional energy dissipation between the adjacent wire helixes inside the EMWM [20]. Moreover, the maximum displacement deviation at the second-order modal frequency is the largest, and that at the third-order modal frequency is the lowest. The maximum displacement deviation at the third-order modal frequency is less than 1.8 μm; thus, the energy dissipation at the third modal frequency can be neglected.

4.3. Thermal-Vibration Joint Test Results and Analysis. During the thermal-vibration joint test, the cantilever structure (baseplate and composite structure with EMWM core) was heated by two quartz lamp infrared heating arrays. Figure 14 shows the preset temperature and control temperature curves on the upper surface of the baseplate for six different thermal environments over the temperature range of 100°C–500°C. As illustrated in Figure 14, the control temperature agrees well with the preset temperature on the

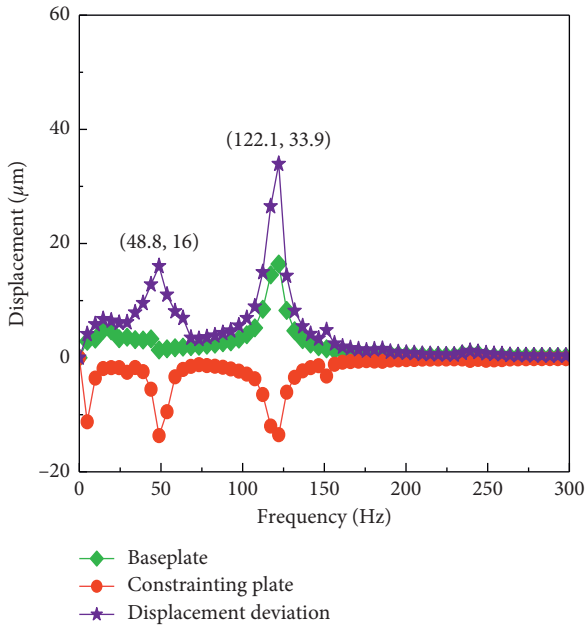

Figure 13: Displacement deviation between the baseplate and the constraining layer (measuring point D1).

Table 7: Maximum displacement deviations of the cantilever composite structure with EMWM core at first three order modal frequencies.

Point	First order		Second order		Third order	
	MV	STD	MV	STD	MV	STD
D1	16.01	0.11	33.92	0.13	1.69	0.01
D2	15.89	0.05	33.68	0.11	1.64	0.02
D3	15.77	0.01	33.38	0.09	1.62	0.02
D4	15.76	0.01	33.27	0.05	1.64	0.01
D5	16.11	0.10	34.03	0.17	1.73	0.02
D6	15.99	0.02	34.01	0.13	1.74	0.01
D7	15.90	0.04	33.83	0.11	1.70	0.02
D8	15.60	0.02	33.41	0.11	1.66	0.01
D9	16.00	0.10	33.93	0.14	1.70	0.02
D10	15.90	0.08	33.58	0.11	1.69	0.02
D11	15.74	0.02	33.50	0.07	1.65	0.02
D12	15.64	0.02	33.36	0.10	1.63	0.01

baseplate in the thermal-vibration joint test. It is noted that the temperature error is within ±4°C.

4.3.1. Effect of Ceramic Extension Rod. In this paper, the ceramic extension rod was made of Al2O3. To investigate the influence of the ceramic extension rod on the modal frequency of cantilever structure, the modal frequency of cantilever structure under the condition of with rod and without rod was measured. Table 8 shows the first three order modal frequencies of the composite structure with/without ceramic extension rod in room temperature environment (25°C). The modal frequencies of the cantilever composite structure with ceramic extension rods are lower than those of the cantilever composite structure without ceramic extension rods. The relative errors of the first three modal frequencies are less than 6%. The test results show that the influence of the ceramic extension rod on the modal frequency of the cantilever composite structure is not significant, which can meet the requirements of engineering applications.

Because the ceramic extension rod has strong deformation resistance at high temperature and high rigidity, the vibration signal loss transmitted through it is small. Therefore, the test result at room temperature can be used as a reference for analyzing the additional mass influence at high temperature.

4.3.2. Modal Frequency. Figure 15 presents the first three order modal frequencies of the cantilever steel plate (baseplate) and cantilever composite structure with EMWM core under different ambient temperatures.

The first three order modal frequencies of the cantilever composite structure with EMWM core are significantly lower than that of the cantilever steel plate (baseplate) in room temperature environment. This phenomenon can be explained by the formula of the natural frequency of vibration with damping, as shown in the following:

$$f_n = \frac{1}{2\pi}\left(\sqrt{\frac{k}{m}}\right)\left(\sqrt{1-\xi^2}\right), \tag{4}$$

where m is mass, k is stiffness, and ζ is damping ratio.

To reduce the vibration of cantilever steel plate (baseplate), an EMWM core, a constraining plate, four limit blocks, and four rivets/bolts were added to the steel plate (baseplate). Therefore, the mass (m) of the composite structure with EMWM core is larger than that of the steel plate (baseplate). Although the stiffness of the EMWM core is less than that of the steel plate (baseplate), for the cantilever composite structure with EMWM core, the clamped end is still part of the steel plate (baseplate), which means that the stiffness (k) of the structure changes a little. It can be seen from Figure 12(c) that the loss factor of EMWM is in the range from 0.08 to 0.14 under different temperatures, while the loss factor of the steel plate is less than 0.02 in room temperature environment [21]. It can be derived from the comparison of the loss factor between steel plate and composite structure with EMWM core that the damping ratio (ξ) of the composite structure is larger than that of the steel plate (baseplate). Therefore, the modal frequencies of the composite structure with EMWM core are lower than the steel plate (baseplate) under room temperature.

The influence of ambient temperature on the modal frequencies of the cantilever composite structure with EMWM core and cantilever steel plate (baseplate) is significant. For the cantilever steel plate, the first three order modal frequencies gradually decrease with the increases of ambient temperature. The main reason for this trend is that the elasticity modulus and stiffness of the steel plate decrease as the temperature increases. For the composite structure with EMWM core, the first three order frequencies are monotonic with the rise of temperature. The changes in the

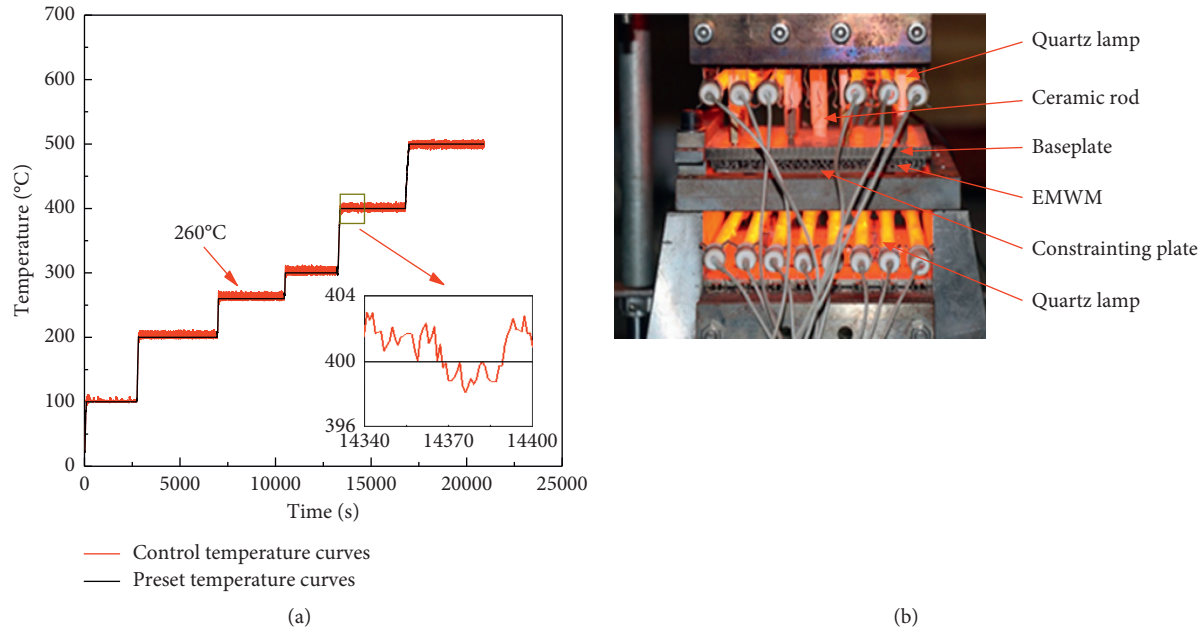

Figure 14: Thermal-vibration joint test. (a) Preset and control temperature on the cantilever structure. (b) Experiment picture.

Table 8: Fist three order modal frequencies of the composite structure with/without ceramic extension rod (25°C).

Condition	Modal frequency (Hz)		
	First order	Second order	Third order
With rod	32.62	128.69	204.97
Without rod	34.57	133.72	216.57
Relative error (%)	5.64	3.76	5.36

first-order modal frequency are relatively small under different temperatures, while the changes in the second-order and third-order modal frequencies become more obvious. It is noted that the second-order modal frequency of the composite structure with EMWM core increases with increasing temperature, and this phenomenon has also been discovered in other studies [22].

4.3.3. Modal Shape. For a vibration system, the low-order resonance energy is higher than the high-order resonance energy, so only the mode shapes of the first three-order resonance frequencies of the plate structure were considered. For a plate structure, its modal shape can be deduced from the comprehensive analysis of the vibration signals, which are obtained by acceleration sensors distributed on the plate structure. In this paper, 12 acceleration sensors were used to detect the vibration signals, and the experimental results for the first three order modal shapes of the cantilever composite structure under different temperatures are presented in Table 9. The first-order and second-order modal shapes are bending modes, and the third-order modal shape is a torsional mode. It can be seen from Table 9 that temperature changes do not cause a change in second- and third-order mode shape. On the other hand, the first-order mode becomes more obvious with the increase of temperature.

4.3.4. Damping Ratio. Figure 16 shows the damping ratio of the composite structure at the first three order modal frequencies under different temperatures. The effect of ambient temperature on the damping ratio of the composite structure with EMWM core is significant. The damping ratio of the composite structure increases first and then decreases with the increase of temperature. Thermal expansion of EMWM core will occur with the increase of temperature. However, the EMWM core is constrained by constraining plate, limit block and bolt. Then the increase of temperature will lead to the reduction of internal porosity of EMWM. During compression, there are three contact states of metal wire helixes in EMWM: noncontact, slip contact, and stick contact [17]. As the temperature increases, the amount of thermal expansion of the wire helixes increases, and then the interaction type of the wire helixes will change gradually (from noncontact to slip, from slip contact to stick contact). It means that the noncontact state occupies a smaller percentage and the number of contact points increases. However, when the wire enters the stuck state, it will not produce sliding friction.

4.3.5. Vibration Reduction of the Cantilever Structure. Frequency response curves (FRCs) of the cantilever baseplate (baseplate) and cantilever composite structure with

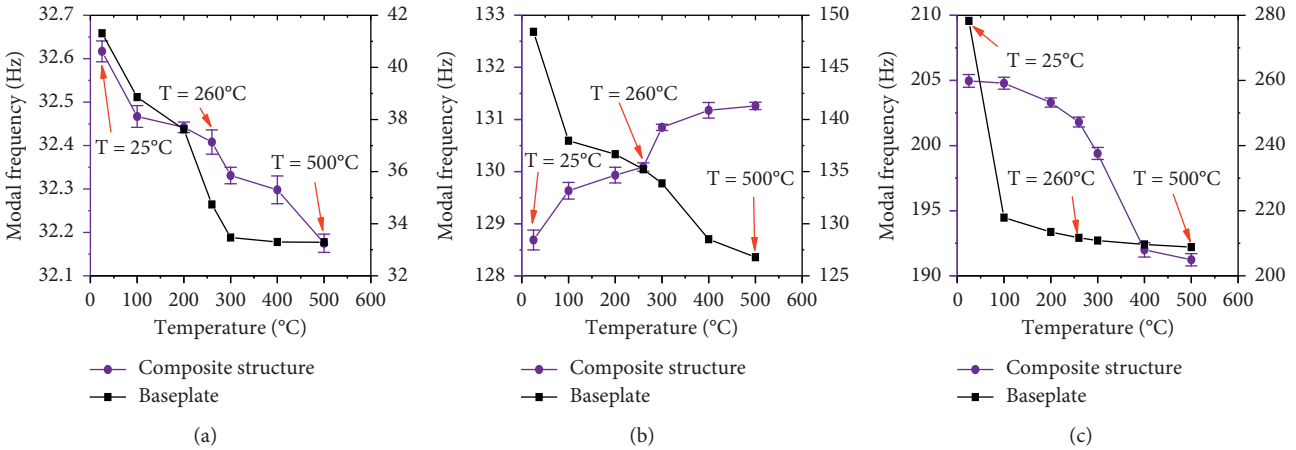

Figure 15: First three order modal frequencies of the cantilever structures under different ambient temperatures. (a) First order. (b) Second order. (c) Third order.

Table 9: First three order modal shapes of the cantilever structure under different temperatures.

Temperature (°C)	First order	Second order	Third order
25		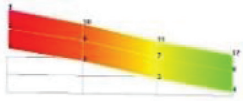	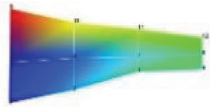
100	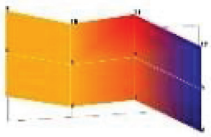	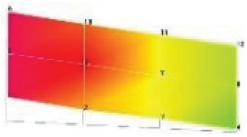	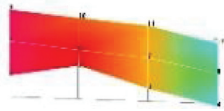
300	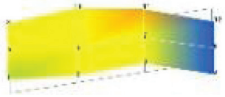	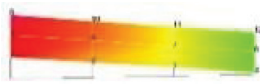	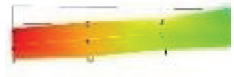
500	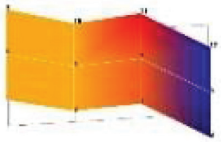	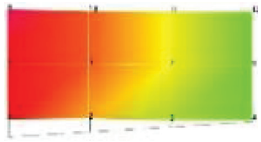	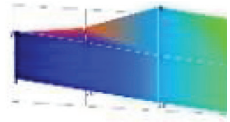

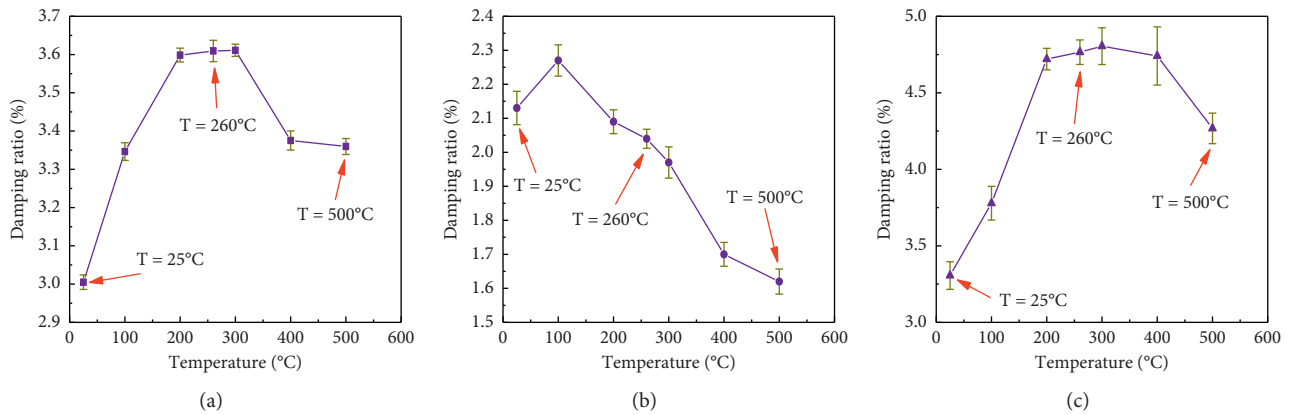

Figure 16: The damping ratio of the composite structure at the first three order modal frequencies under different temperatures. (a) First order. (b) Second order. (c) Third order.

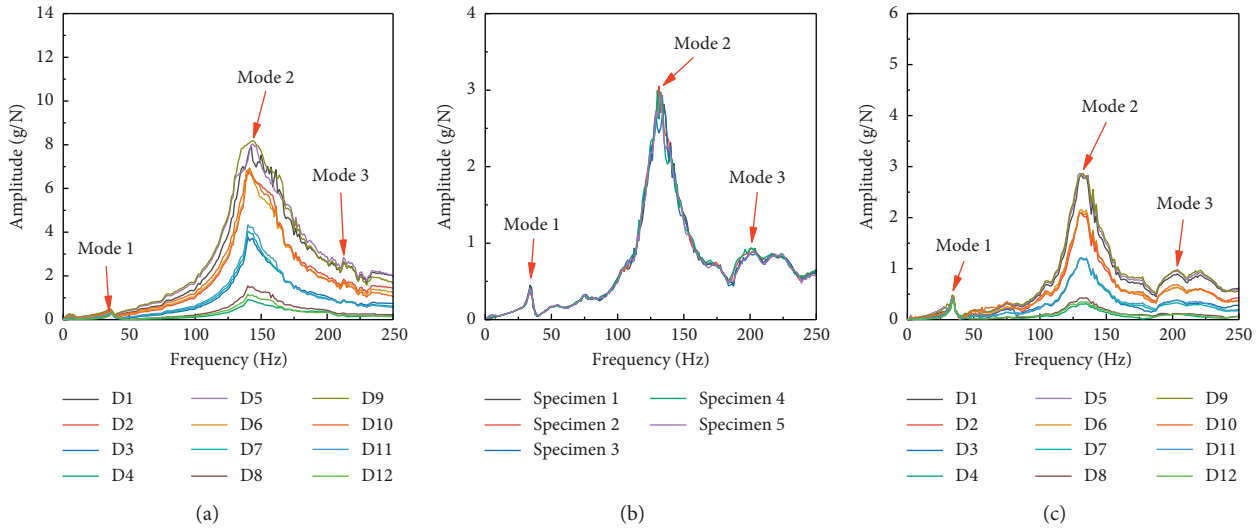

Figure 17: The frequency response curves (FRCs) of baseplate and composite structure with EMWM core. (a) The FRCs for baseplate at different measure points. (b) The FRCs for composite structure with different core at measure point D1. (c) The FRCs for composite structure at different measure points under room temperature.

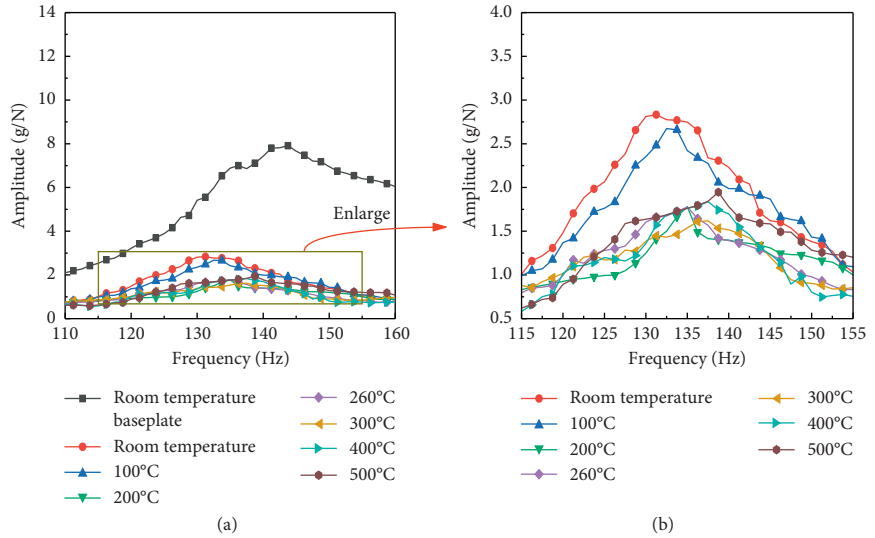

Figure 18: Frequency response curves of cantilever structure under different temperatures. (a) Second-order FRCs and (b) drawing of second-order FRCs.

EMWM core were obtained by signal source and data acquisition system (uT8916FRS-DY) in real time. Figure 17(a) shows the FRCs of the cantilever baseplate (steel plate) at different measuring points. The amplitude at the second-order modal frequency was larger than the orders. Figure 17(b) presents the FRCs of composite structure with EMWM cores at measure point D1 under room temperature. The consistency of these samples is high. To facilitate the analysis of the effect of temperature on the vibration reduction of the cantilever structure, one of these specimens was selected and compared with the baseplate under different high temperatures. Figure 17(c) shows the FRCs of a composite structure with EMWM core at different measure points. The shape of the curves is similar to that in Figure 17(a). It can be clearly seen from Figures 17(a) and 17(c) that, under the same excitation condition, the maximum amplitude (2.815 g/N) of the cantilever composite structure at room temperature at measuring point D1 is 64.41% lower than that of the cantilever baseplate (steel plate) (7.909 g/N). It means that the vibration amplitude of the cantilever plate structure can be greatly reduced by using metal damping materials (EMWM).

To investigate the vibration reduction of cantilever structure under different temperatures, Figure 18(a) presents the frequency response curves of cantilever structure under different temperatures. Figure 18(b) is the drawing of partial enlargement of Figure 18(a). The vibration amplitude of the cantilever structure under different high temperatures is reduced compared to that under room temperature. However, there is no significant difference in the effect of

vibration reduction between 200°C and 500°C. This is consistent with the second-order damping ratio of the composite structure in the same temperature range. It means that the vibration of the cantilever steel plate (baseplate) can be reduced under different temperature by adding EMWM core and constraining plate.

5. Conclusions

A new composite structure with EMWM core was proposed for reducing vibration of cantilever steel plate in high-temperature environments. The damping mechanism of this composite structure was validated by detecting the displacement deviation between the baseplate and constraining plate. A thermal-vibration joint test system was set up to investigate the vibration and damping characteristics of a cantilever composite structure with EMWM core. The main conclusions, which can be drawn from the conducted experiments, are as follows:

(1) The energy dissipation characteristic of EMWM is not affected by temperature below 260°C. Although the energy dissipation characteristic of EMWM decreases after the temperature exceeds 260°C, it still has dissipation capacity.

(2) The displacement deviations between the baseplate and constraining plate are sufficient to cause frictional energy dissipation between the internal adjacent wire helixes.

(3) The vibration of the cantilever steel plate can be significantly reduced by adding EMWM core and constraining plate in the wide temperature range (from room temperature to 500°C).

Data Availability

The data used to support the findings of this study are available from the corresponding author upon request.

Conflicts of Interest

The authors declare that they have no conflicts of interest.

Acknowledgments

This work was supported by the National Natural Science Foundation of China (Grant no. 51805086).

References

[1] L. Irazu and M. J. Elejabarrieta, "The influence of viscoelastic film thickness on the dynamic characteristics of thin sandwich structures," *Composite Structures*, vol. 134, pp. 421–428, 2015.

[2] H. B. Bai, C. H. Lu, and F. L. Cao, *Metal Rubber Material and Engineering Application*, Science Press, Beijing, China, 2014.

[3] K. A. Wu, H. B. Bai, X. Xue, T. Li, and M. Li, "Energy dissipation characteristics and dynamic modeling of the coated damping structure for metal rubber of bellows," *Metals*, vol. 8, 2018.

[4] Y. H. Ma, X. L. Tong, B. Zhu, D. Y. Zhang, and J. Hong, "Theoretical and experimental investigation on thermophysical properties of metal rubber," *Acta Physica Sinica*, vol. 62, p. 10, 2013.

[5] J. Hu, Q. Du, J. Gao, J. Kang, and B. Guo, "Compressive mechanical behavior of multiple wire metal rubber," *Materials & Design*, vol. 140, pp. 231–240, 2018.

[6] P. Yang, H. Bai, X. Xue, K. Xiao, and X. Zhao, "Vibration reliability characterization and damping capability of annular periodic metal rubber in the non-molding direction," *Mechanical Systems and Signal Processing*, vol. 132, pp. 622–639, 2019.

[7] Y. B. Lee, C. H. Kim, T. H. Kim, and T. Y. Kim, "Effects of mesh density on static load performance of metal mesh gas foil bearings," *The Journal of Engineering for Gas Turbines and Power*, vol. 134, 2012.

[8] S.-C. Kwon, S.-H. Jeon, and H.-U. Oh, "Performance evaluation of spaceborne cryocooler micro-vibration isolation system employing pseudoelastic SMA mesh washer," *Cryogenics*, vol. 67, pp. 19–27, 2015.

[9] K. Chandrasekhar, J. Rongong, and E. Cross, "Mechanical behaviour of tangled metal wire devices," *Mechanical Systems and Signal Processing*, vol. 118, pp. 13–29, 2019.

[10] K. Xiao, H. B. Bai, X. Xue, and Y. W. Wu, "Damping characteristics of metal rubber in the pipeline coating system," *Shock and Vibration*, vol. 2018, Article ID 3974381, 11 pages, 2018.

[11] Y. Zhu, Y. W. Wu, H. B. Bai, Z. Y. Ding, and Y. C. Shao, "Research on vibration reduction design of foundation with entangled metallic wire material under high temperature," *Shock and Vibration*, vol. 2019, Article ID 7297392, 16 pages, 2019.

[12] J. F. Hou, H. B. Bai, and D. W. Li, "Damping capacity measurement of elastic porous wire-mesh material in wide temperature range," *Journal of Materials Processing Technology*, vol. 206, no. 1–3, pp. 412–418, 2008.

[13] T. Li and H. B. Bai, "Compressive property of knitted-dapped metal rubber at different temperature," *Materials for Mechanical Engineering*, vol. 42, pp. 58–61, 2018.

[14] Z. Y. Ding, H. B. Bai, Y. W. Wu, Y. Zhu, and Y. C. Shao, "Experimental Investigation of Thermal Modal Characteristics for a Ship's Foundation under 300°C," *Shock and Vibration*, vol. 2019, Article ID 2714930, 11 pages, 2019.

[15] L. Zheng, D. Wu, B. Pan, Y. Wang, and B. Sun, "Experimental investigation and numerical simulation of heat-transfer properties of metallic honeycomb core structure up to 900 °C," *Applied Thermal Engineering*, vol. 60, no. 1-2, pp. 379–386, 2013.

[16] B. Gadot, O. Riu Martinez, S. Rolland du Roscoat, D. Bouvard, D. Rodney, and L. Orgéas, "Entangled single-wire NiTi material: a porous metal with tunable superelastic and shape memory properties," *Acta Materialia*, vol. 96, pp. 311–323, 2015.

[17] Y. H. Ma, W. Z. Hu, D. Y. Zhang, Q. C. Zhang, and J. Hong, "Tunable mechanical characteristics of a novel soft magnetic entangled metallic wire material," *Smart Materials and Structures*, vol. 25, 2016.

[18] R. K. Desu, H. Nitin Krishnamurthy, A. Balu, A. K. Gupta, and S. K. Singh, "Mechanical properties of austenitic stainless steel 304L and 316L at elevated temperatures," *Journal of Materials Research and Technology*, vol. 5, no. 1, pp. 13–20, 2016.

[19] Z. Y. Ding, H. B. Bai, Y. W. Wu, Z. Y. Ren, and Y. C. Shao, "A constitutive model of plate-like entangled metallic wire material in wide temperature range," *Materials*, vol. 12, 2019.

[20] Y. Y. Wang, H. B. Bai, and Y. F. Liu, "Micro characteristic study of the compressive performance of metal rubber

material," *Mechanical Science and Technology for Aerospace Engineering*, vol. 30, pp. 404–407, 2011.

[21] J. Zhang, R. J. Perez, and E. J. Lavernia, "Documentation of damping capacity of metallic, ceramic and metal-matrix composite materials," *Journal of Materials Science*, vol. 28, no. 9, pp. 2395–2404, 1993.

[22] Y. W. Wang, "Study on the thermal-vibration characteristics for wing structures of high-speed flight vehicle," *School of Aeronautic Science and Engineering*, Beihang University, Beijing, China, 2013.